Supplemental materials

CD11c regulates neutrophil maturation

Short title: CD11c and neutrophil maturation

Lifei Hou[1,2], Richard A. Voit[3], Miho Shibamura-Fujiogi[1,2], Sophia Koutsogiannaki[1,2], Yunan Li, M.S.[4], Yue Chen, Ph.D.[4], Hongbo Luo[5], Vijay G. Sankaran[3], Koichi Yuki[1,2,*]

[1]Department of Anesthesiology, Critical Care and Pain Medicine, Cardiac Anesthesia Division, Boston Children's Hospital, Boston, MA, USA

[2]Department of Anaesthesia and Immunology, Harvard Medical School, Boston, MA, USA

[3]Department of Hematology/Oncology, Boston Children's Hospital and Department of Pediatric Oncology, Dana-Farber Cancer Institute, Harvard Medical School, Boston, MA, USA

[4]Department of Biochemistry, Molecular Biology and Biophysics, University of Minnesota

[5]Department of Pathology, Boston Children's Hospital, Boston, MA, USA

Supplemental Methods

Neutrophil differentiation of 32Dcl3 and HL-60 cells

32Dcl3 cells were a kind gift from Dr. Morris White (Boston Children's Hospital). 32Dcl3 cells were maintained in complete RPMI-1640 medium supplemented with 10%FCS, 2 mM L-glutamine, 10 mM HEPES, 1 mM sodium pyruvate, 50 μM 2-mercaptoethanol (ME), 1% penicillin/streptomycin and 1 ng/ml murine IL-3 (PeproTech; Rocky Hill, NJ). They were differentiated with G-CSF (100 ng/mL) for 7 days as previously described [1]. HL-60 cells were obtained from ATCC (Manassas, VA) and maintained in complete RPMI-1640 medium supplemented with 10% FCS, 2 mM L-glutamine, 10 mM HEPES, 1 mM sodium pyruvate, 50 μM 2-ME and 1% penicillin/streptomycin. HL-60 cells were differentiated with 1 μM all-trans retinoic acid (ATRA, Sigma-Aldrich; St. Louis, MO) and 1.25% DMSO for 4 days. Neutrophil differentiation was confirmed with Giemsa staining. For HL-60 cells, surface CD11b was also monitored as a marker for differentiation and maturation [2].

HL-60 derived neutrophils and CRISPR/Cas9 gene editing

CRISPR/Cas9 editing to delete CD11c expression was done in HL-60 cells as follows. HL-60 cells were cultured at 37ºC in RPMI1640 supplemented with 10% FBS, 1% penicillin/streptomycin. Confluency was maintained between 3 $x10^5$-1.5x 10^6/ml. Electroporation was performed one day after passaging when cells were in log phase of growth using the Lonza 4D Nucleofector with 20 μl Nucleocuvette strips as described [3,4]. Briefly, ribonucleoprotein (RNP) complex was made by combining 100 pmol Cas9 (IDT; Newark, NJ) and 100pmol modified sgRNA (Synthego; Redwood City, CA) targeting ITGAX using either sg1 (GAAACCUAGAGAAGUUGCUA) or

sg2 (CCAGCCUUAGCAACUUCUCU) and incubating at room temperature for 15 minutes. As a control, sgRNA targeting AAVS1 was used (GGGGCCACTAGGGACAGGAT).

2 x10^5- 4 x 10^5 HL-60 cells were resuspended in 20 µl SF cell line solution (Lonza; Basel, Switzerland) and were mixed with RNP and underwent nucleofection with program EN-138 as per manufacturer recommendations. Cells were returned to RPMI1640 media and editing efficiency was measured 48 hours after electroporation by polymerase chain reaction (PCR). First, genomic DNA was extracted using the DNeasy kit (Qiagen; Hildgen, Germany) according to the manufacturer's instructions. Genomic PCR was performed using Platinum II Hotstart Mastermix (Thermo Fischer Scientific) and edited allele frequency was detected by Sanger sequencing and analyzed by ICE [5], The following primer pairs were used: ITGAX (forward: GCGCCAACTTGTGCTCTGTGGA; reverse: CAGCACTTTGGGAGGCTGAGGC), AAVS1 (forward: TTCGGGTCACCTCTCACTCC; reverse: GGCTCCATCGTAAGCAAACC). Single cell-derived colonies following ITGAX editing were obtained by performing limiting dilution into a 96-well plate. Single cells were expanded, and genotyping of colonies was performed by Sanger sequencing as above. Colonies were found to have one of the following genotypes: homozygous wild type, homozygous knockout, or compound heterozygous with one out of frame edit and one in-frame edit. No heterozygous colonies were isolated.

Neutrophil extracellular traps (NETs) formation.

Bone marrow neutrophils (2.5 × 10^5 in 200 µl) in RPMI 1640 with 10 mM HEPES and 50 µM 2-ME were allowed to adhere to eight-well glass chamber slides (Thermo Fisher Scientific) for 1 h at 37°C followed by phorbol-12-myristate-13-acetate (PMA) (50 nM) for 4 h. To quantify NETs, the cells at the termination of NET induction were washed once with warm PBS, and then Sytox

green (0.1 μM) was added. The NETs were imaged with a fluorescence microscope, Zeiss Axiovert (Carl Zeiss; Thornwood, NY).

Reactive oxygen species [6]

Mouse neutrophils (2×10^5 in 200 μl) were cultured in complete RPMI 1640 at 37°C for 30 min. Dihydrorhodamine-123 (1 μM; Sigma-Aldrich) was added for 5 min at 37°C. Neutrophils were washed once. PMA (100 nM) was added, and the cells were incubated for additional 15 min at 37°C. After one wash, the cells were resuspended in cold PBS with 1% FCS for detection of ROS-induced rhodamine-123 on a FACSCanto (BD Biosciences). Regarding HL-60-derived neutrophils, they were cultured in RPMI 1640 with 2% heat-inactivated FBS at 37°C for 30 min in the presence of PMA (100 nM) **[6]**.

Phagocytosis

The neutrophil phagocytosis was done using Phagotest Kit (Glycotope Biotechnology; Heidelberg, Germany). Mouse neutrophils or HL-60-differentiated neutrophils were cultured in complete RPMI 1640 on ice for 10 min, followed by the addition of FITC-*E. Coli*. Then the neutrophil suspension was kept on ice as cold control or was put into 37°C water bath for 10 min. At the end of incubation, cells were transferred back on ice, quenched, and washed. Cells were suspended in PBS/1% PFA and measured by FACSCanto (BD Biosciences) and analyzed by FlowJo software (Tree Star).

Neutrophil chemotaxis assay

Bone marrow neutrophils were subjected to horizontal chemotaxis assay using the EZ-TAXIScan apparatus (Effector Cell Institute; Tokyo, Japan) as previously performed [7]. Neutrophils suspended in RPMI1640 containing10 mM HEPES, 0.1% BSA and 10 mM EDTA

were aligned on one edge of the chemotaxis channel. At the other end, 1 μM N-formylmethionine-leucyl-phenylalanine (fMLP) was injected, creating a gradient along the channel. Pictures were taken every 30 seconds for 20 min, and recorded movies were analyzed using FIJI software (National Institute of Health; Bethesda, MD).

Proliferation and apoptosis analysis.

In vivo proliferation of cells was examined by BrdU incorporation. Mice were injected intraperitoneally (*i.p.*) with 1 mg of BrdU. To detect BrdU incorporation into bone marrow hematopoietic cells, BD cytofix/cytoper^{TM} Plus kit (BD Bioscience) and Alexa Fluor488-conjugated anti-BrdU antibody (3D4, Biolegend) were applied according to the manufacture's protocol. Cells were subjected to flow cytometry analysis. Apoptosis was detected with intracellular staining of active caspase-3 antibody (BD Biosciences).

CyTOF assay.

After red blood cell lysis, bone marrow cells were collected and resuspended in cell staining buffer (Fluidigm; San Francisco, CA). After centrifugation, Fc receptor blocking reagent (clone 93, Biolegend) was used at a 1:100 dilution in for 10 minutes, followed by incubation with the metal conjugated surface antibodies listed below (except cleaved caspase 3 and Ki67 antibodies) for 30 minutes. Then the cells were fixed and permeabilized by using fixation/permeabilization reagents (BD Bioscience), followed by staining with metal labeled cleaved caspase 3 and Ki67 antibodies. The permeabilization buffer was made by diluting the 10x stock solution (51-2091, BD Biosciences) in UltraPure distilled water (Invitrogen). All antibodies were purchased from the CyTOF core facility at Brigham and Women's Hospital. Antibodies used were as follow; Ly6C (HK1.4)-112Cd, B220 (RA3-6B2)-113In, CD8a (53-6.7)-116Cd, IgM (RMM-1)-142Nd,

Ter-119-143Nd, CD184 (L276F12)-144Nd, CD11c (N418)-146Nd, CD127 (A7R34)-148Nd, CD19 (6D5)-149Sm, CD11b (M1/70)-150Nd, CD48 (HM48-1)-154Sm, Cleaved caspase 3 (D3E9)-156Gd, Ly6G (1A8)-158Gd, Ly6A/E (E13-161.7)-160Gd, CD135 (A2F10)-162Dy, CD3 (145-2C11)-152Sm, CD48 (Rm4-5)-115ln, CD182 (242216)-165Ho, CD34 (MEC14.7)-166Er, CD117 (2B8)-168Er, Siglec-F (E50-2440)-170Er, CD150 (TC15-12F12.2)-171Yb, Ki-67 (8D5)-161Dy. DNA was labeled with iridium intercalator solution (Fluidigm). Samples were subsequently washed and reconstituted in Milli-Q filtered distilled water in the presence of EQ Four Element Calibration beads (Fluidigm, catalog 201078). Samples were acquired on a Helios CyTOF Mass Cytometer (Fluidigm) at Cellular Profiling Core Facility (School of Public Health, Harvard Medical School, Boston, MA, USA); Data were analyzed by using spanning-tree progression analysis of density-normalized events (SPADE) and visualization of t-distributed stochastic neighbor embedding (SNE) on Cytobank software.

Western blot.

Immature and mature neutrophils were sorted from BM cells using FACSAria and subjected to Western blot analysis. Protein samples were resolved by Tris-glycine gels and transferred onto PVDF membrane. After blocking in 5% non-fat dry milk, the membranes were incubated with anti-myeloperoxidase (MPO, sc33596, Santa Cruz Biotech; CA, USA), anti-matrix metallopeptidase 9 (MMP9, sc393859, Santa Cruz Biotech; Santa Cruz, CA), ant-Serpin B1 (rabbit polyclonal antiserum, kindly provided by Dr. Eileen Remold-O'Donnell, Boston Children's Hospital), and anti-GAPDH (2118, Cell signaling) antibodies. Membranes were then incubated with respective secondary antibodies labeled with horseradish peroxidase (HRP). Immunoreactive proteins were visualized by enhanced chemiluminescence (Thermo Fischer Scientific).

Systemic LPS challenge or E. coli infection model

Mice were subjected to LPS (10 mg/kg) *i.v.* injection or *Escherichia coli* (*E. coli*)-GFP (ATCC 25922-GFP, 10^8 CFU) intraperitoneal (*i.p.*) injection. Mice were euthanized at different time points for analysis. Regarding *E. coli* infection model, *E. coli* GFP was overnight cultured in Luria-Bertani [8] ampicillin (100 μg/ml) medium at 37°C and washed twice with sterile PBS buffer. Peritoneal fluid was collected by lavage using 5 ml of cold PBS buffer. Serial dilutions of the final bacterial inocula were plated on LB-ampicillin (100 μg/ml) agar plates and incubated overnight at 37°C to verify the number of live bacteria injected. Bacterial loads in peritoneal lavage fluid (PLF) were determined by plating serial dilutions of each sample on LB-ampicillin agar plates overnight at 37°C and counting the number of CFU.

Chimeric mouse experiments

To generate mixed bone marrow chimeras, recipient mice on the C57BL/6 background were irradiated with two doses of 550 rad with 4-hour intervals. Wild-type (WT; CD45.1) and CD11cKO (CD45.2) derived bone marrow cells were separately injected (single chimera) or mixed at the ratio of 1:9 and injected (mixed chimera) into the tail vein of lethally irradiated recipients. Total of 5×10^6 cells were injected. Mice were evaluated for the reconstitution of the immune compartment at various time points after bone marrow transplantation. To prevent bacterial infection, the mice were provided with autoclaved drinking water containing Sulfatrim for 1 week prior to and for 4 weeks after irradiation.

Rosetting assay

Bone marrow cells were obtained and cultured in 6 well plates in RPMI1640 supplemented with 10% heat inactivated FBS, glutamine, penicillin, streptomycin, GM-CSF (20 ng/mL) and IL-4 (5

ng/mL). At day 3, the culture medium was entirely discarded and replaced with freshly warmed medium containing GM-CSF and IL-4. At day 7, cells were subjected to rosetting assay as previously described [9]. Briefly, sheep erythrocytes were sensitized with iC3b by co-incubating with anti-sheep erythrocyte stroma antibody (M1/87) followed by C5-deficient human serum as previously described [10]. Opsonized sheep erythrocytes were given to each well with 1 mM Mg^{2+}/Ca^{2+} or 1 mM Mn^{2+} and incubated at 37ºC for 1 hour. Wells were washed three times and subjected to microscopic examination. Rosettes were considered when > 10 erythrocytes were on a cell.

GST-CD11c I domain purification

Recombinant human CD11c I domain containing I333G mutant was cloned into pGEX-2T vector and expressed on Escherichia coli BL21 (DE3) [11]. Bacterial cells were cultured in LB with 0.5 mM isopropyl β-D-thiogalactopyranoside (IPTG) stimulation. GST-tagged CD11c I domain I333G was purified with glutathione sepharose bead column as previously described [12].

Mass spectrometry analysis

Proteins associated with activated CD11c I domain were examined by pulling down HL-60 cell lysates using GST-tagged human CD11c I domain I333G. Following glutathione sepharose bead pull-down, proteins were resolved on SDS-PAGE and stained by Coomassie blue followed by in-gel tryptic digestion as previously described[13]. Extracted peptide samples were analyzed by the nano-flow liquid chromatography coupled to an Orbitrap Fusion mass spectrometry (nLC-MS/MS, Thermo Scientific) using a Proxeon Easy nLC 1000 Nano-UPLC system (Thermo Scientific) with a Top-12 data-dependent acquisition (DDA) as previously described [13]. Peptides were injected onto an in-house packed reversed-phase capillary HPLC column of 15 cm x 100

µm (RP-C18, ReproSil-Pur Basic C18, 2.5 µm) after re-solubilization in HPLC buffer A (0.1% formic acid in water (v/v)). The peptides were separated by HPLC buffer B (0.1% formic acid (v/v)), a 90 min gradient of 7-32% acetonitrile at a flow rate of 200 nL/min. Full scan of precursor ions (MS1) were performed with a resolution of 60K at a mass range of 380 – 1580 m/z in a positive mode. A mass tolerance of ± 10 ppm was applied in dynamic exclusion of 15 s. Fragment ions (MS2) were performed using an isolation window of 1.6 m/z along with collision-induced dissociation (CID) energy of 35% in the linear ion trap. Raw mass spectra data were analyzed by MaxQuant searching software (version 1.5.3.12) coupled to the integrated Andromeda search engine [14,15]. Peptides and proteins were identified with a statistics-based scoring algorithm and filtered at 1% false discovery rate (FDR) by searching against the UniProt human database (downloaded 19 September 2018) in concatenation with the reversed decoy database. Mass tolerance in full MS spectra was set to +/- 4.5 ppm and mass tolerance in MS/MS spectra was set to +/-0.5 Da. Trypsin was specified as the enzyme with a maximum missed cleavage of 2. Fixed modification includes cysteine carbamidomethylation, and variable modifications include methionine oxidation and protein N- acetylation. Top hit proteins were subjected to STRING software (https://string-db.org) for protein-protein interaction.

CD11c immunoprecipitation

HL-60 cells, differentiated HL-60 cells, 32Dcl3 cells, and differentiated 32Dcl3cells were collected and lysed on ice in RIPA buffer (Thermo Fisher Scientific) for 30 min, centrifuged (15,700 *g*, 4°C, for 5 min) and the supernatant was collected. To deplete non-specific binding, 1 µg control IgG and 20 µl of Protein A+G conjugated beads (SC2003, Santa Cruz Biotech, CA, USA) were added into the supernatant and incubated at 4°C for 30 minutes, followed by centrifugation. Then the cell lysates were incubated with anti-human CD11c mAb (CBRp150

2c1) overnight in 4°C. Protein A+G conjugated beads were added and incubated in 4°C for 2 hours. The beads were extensively washed and boiled in SDS-loading buffer, the supernatants were separated by 4-20% Tris-glycine gels and transferred onto PVDF, followed by Western blot analysis using IQGAP1 antibody (2293, Cell signaling) or polyclonal anti-CD11c antibody (PA5-90208, Invitrogen).

RNA sequencing experiments

Freshly sorted mature neutrophil or immature neutrophils stimulated under G-CSF (100 ng/mL) after sorting were subjected to RNA purification using Qiagen RNeasy Plus Mini Kits. RNA samples were quantified using Qubit 2 Fluorometer (Life Technology; Carlsbad, CA) and RNA integrity was checked with Agilent TapeStation (Agilent Technologies; Palo Alto, CA). SMART-Seq v4 Ultra Low Input kit for Sequencing was used for full-length cDNA synthesis and amplification (Clonetech; Mountain View, CA), and Illumina Nextera XT library was used for sequencing library preparation. Briefly, cDNA was fragmented, and adaptor was added using transposase, followed by limited-cycle PCR to enrich and add index to the cDNA fragments. The final library was assessed with Qubit 2.0 Fluorometer and Agilent TapeStation. The sequencing libraries were multiplexed and clustered on one lane of a flowcell. After clustering, the flowcell was loaded on the Illumina HiSeq instrument according to the manufacturer's instructions. The samples were sequenced using a 2x150 paired end configuration. After investigating the quality of the raw data, sequencing reads were trimmed to remove possible adapter sequences and nucleotides with poor quality using Trimmomatic v.0.36. The trimmed reads were mapped to the mouse reference genome using STAR aligner v.2.5.2b. Only unique reads that fell within exon regions were counted. After extraction of gene hit counts, the gene hit counts table was used.

Using DESeq2, a comparison between the groups of samples was performed. The Wald test was used to generate p-value and Log2 fold changes. Genes with adjusted p-values < 0.05 and absolute log2 fold change > 1 were called differentially expressed genes. Ontology analysis was performed using Ingenuity Pathway Analysis (IPA) software (Qiagen).

Nuclear extraction of neutrophils.

Mouse neutrophils were isolated by Percoll gradient with purity >90%. The nucleus of neutrophils was isolated according to the method described by McCaffrey *et al*. with slight modification [16]. In brief, neutrophils were washed with saline, and then resuspended (5×10^6/ml) in hypotonic buffer (10 mM Tris, 10 mM NaCl, 3 mM $MgCl_2$) containing 0.5% NP40, 2 mM AEBSF and 50 μg/ml Leupeptin. Cells were placed on ice for 10 minutes and nuclei were collected by centrifugation (6000 *rpm*, 5min, 4 ^oC) and washed with the same buffer without NP40. After extraction, both nuclei and supernatant were dissolved by SDS sample buffer and further analyzed by western blot analysis.

Supplemental Figures

Supplemental Figure 1.

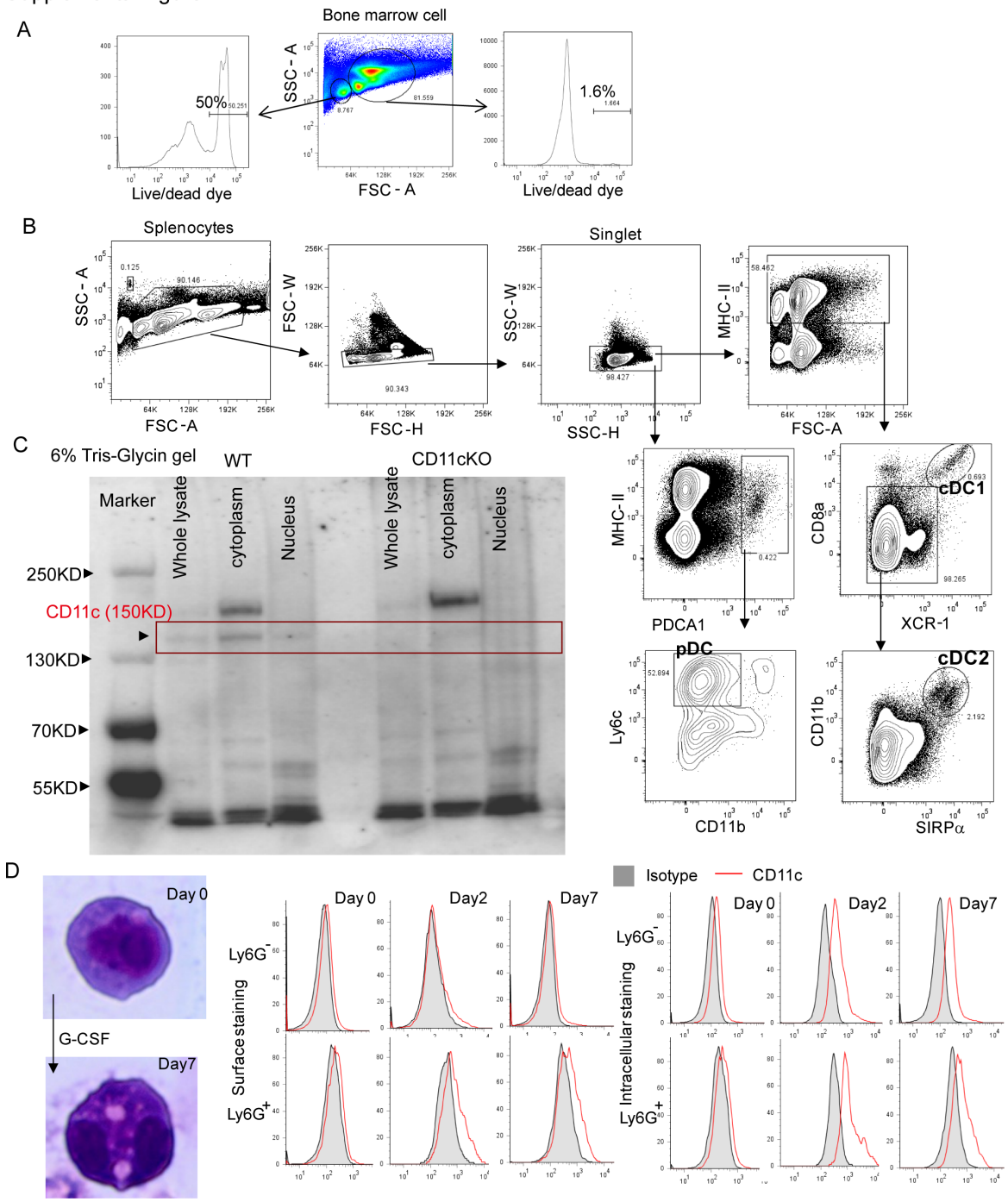

Supplemental Figure1. CD11c expression on mouse neutrophils differentiated from 32D cell line. A. Live/Dead staining of bone marrow cells. **B**. Gating strategy of splenic dendritic cells. Spleens from WT mice were digested with collagenase-IV (0.5 mg/ml) and DNase (50U/ml) for 20 min in RPMI-1640 containing 5%FBS, and then washed, subjected to red blood cell lysis, and made into single cell suspension. Flow cytometric photos showed the gating strategy for identifying the cDC1 (MHC-II^{hi}CD8α^{+}XCR-1^{+}) and cDC2 (MHC-II^{hi}CD8α^{-}XCR-1^{-}

$CD11b^{+}SIRP\alpha^{+}$) and pDC ($MHC\text{-}II^{+}PDCA1^{+}Ly6C^{+}CD11b^{-}$) subsets. Shown is a representative flow cytometry picture from at least 5 independent experiments. **C,** CD11c detection (polyclonal anti-CD11c antibody, PA5-90208, Invitrogen) of whole cell lysate, cytoplasm, and nucleus of mouse neutrophils isolated from bone marrow. Both WT and CD11cKO mice were used. Shown is one of two repeats with the same pattern. **D,** Left: Giemsa staining of 32Dcl3 cell before and post differentiation into neutrophils. Right: flow cytometry overlay analysis showing the surface expression (middle panel) and intracellular expression (bottom panel) of CD11c on 32Dcl3 cells under differentiation stimulant (G-CSF) into neutrophils. Shown are representative data from five experiments with same pattern.

Supplemental Figure 2.

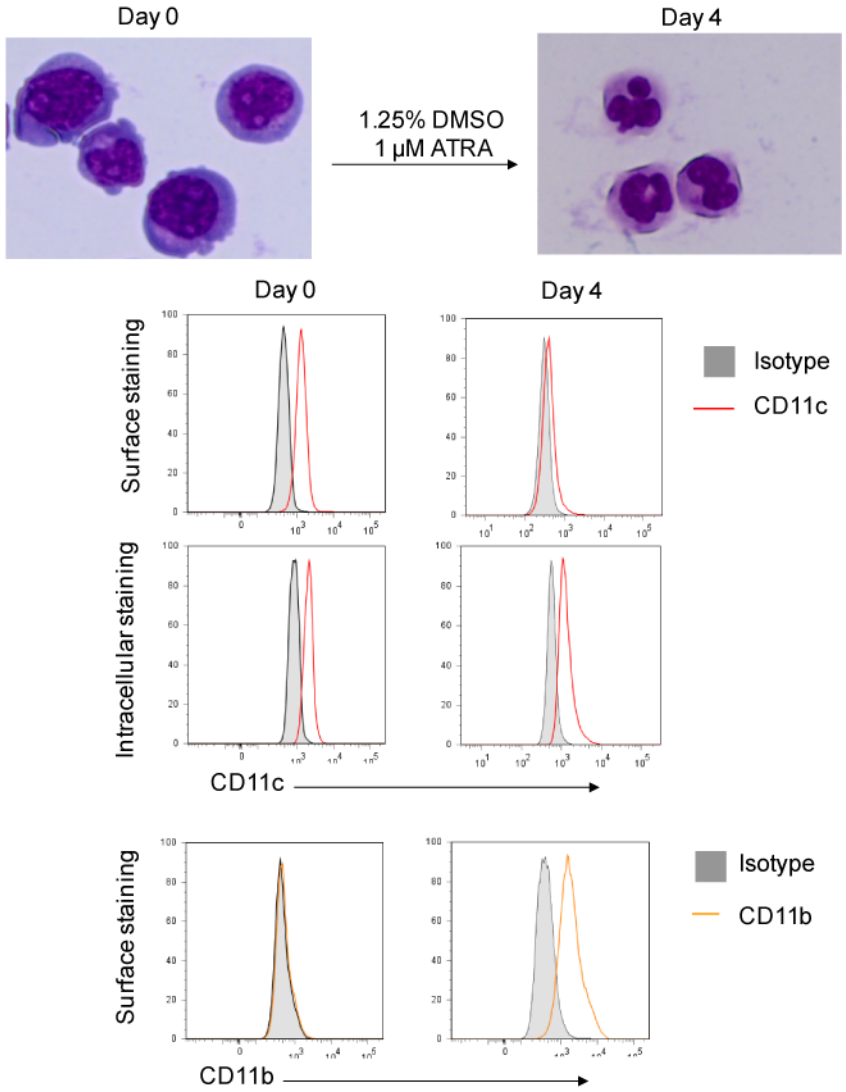

Supplemental Figure 2. CD11c expression on human neutrophils differentiated from HL-60 cell line. Top panel**:** Giemsa staining of HL-60 cells before and post differentiation into neutrophils. Middle panel: flow cytometry overlay analysis showing the surface expression and intracellular expression of CD11c on HL-60 cells under differentiation stimulants (DMSO, retinoic acid) into neutrophils. Bottom panel: CD11b expression on HL-60 cells before and after differentiation into neutrophils.

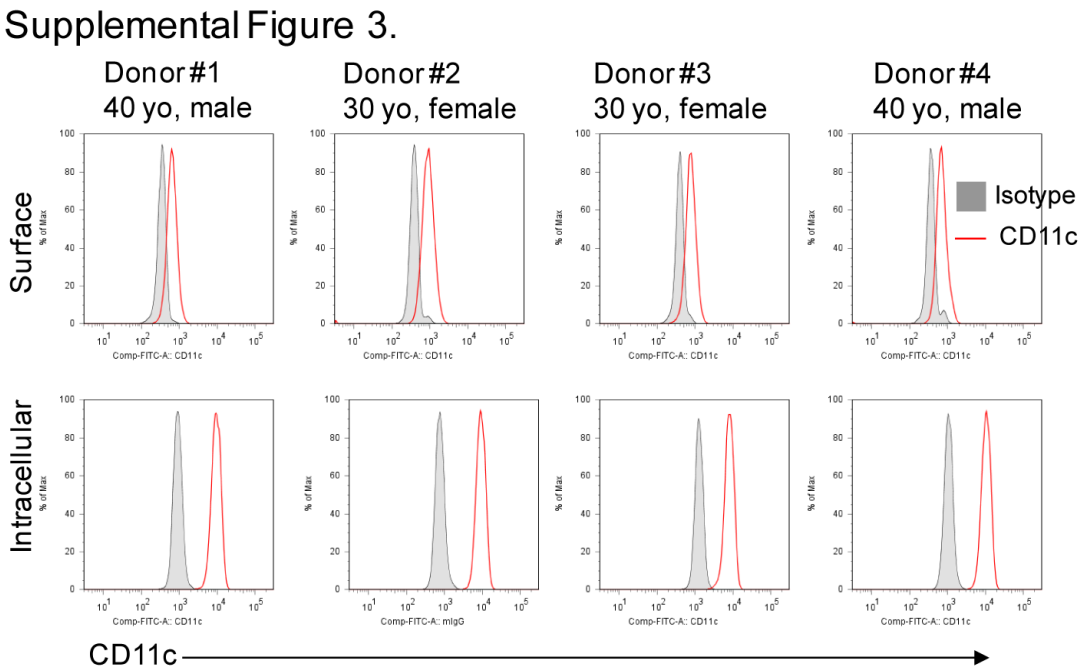

Supplemental Figure 3. CD11c expression on human neutrophils isolated from peripheral blood. Both surface and intracellular CD11c expressions were measured by flow cytometry using four independent donors.

Supplemental Figure 4.

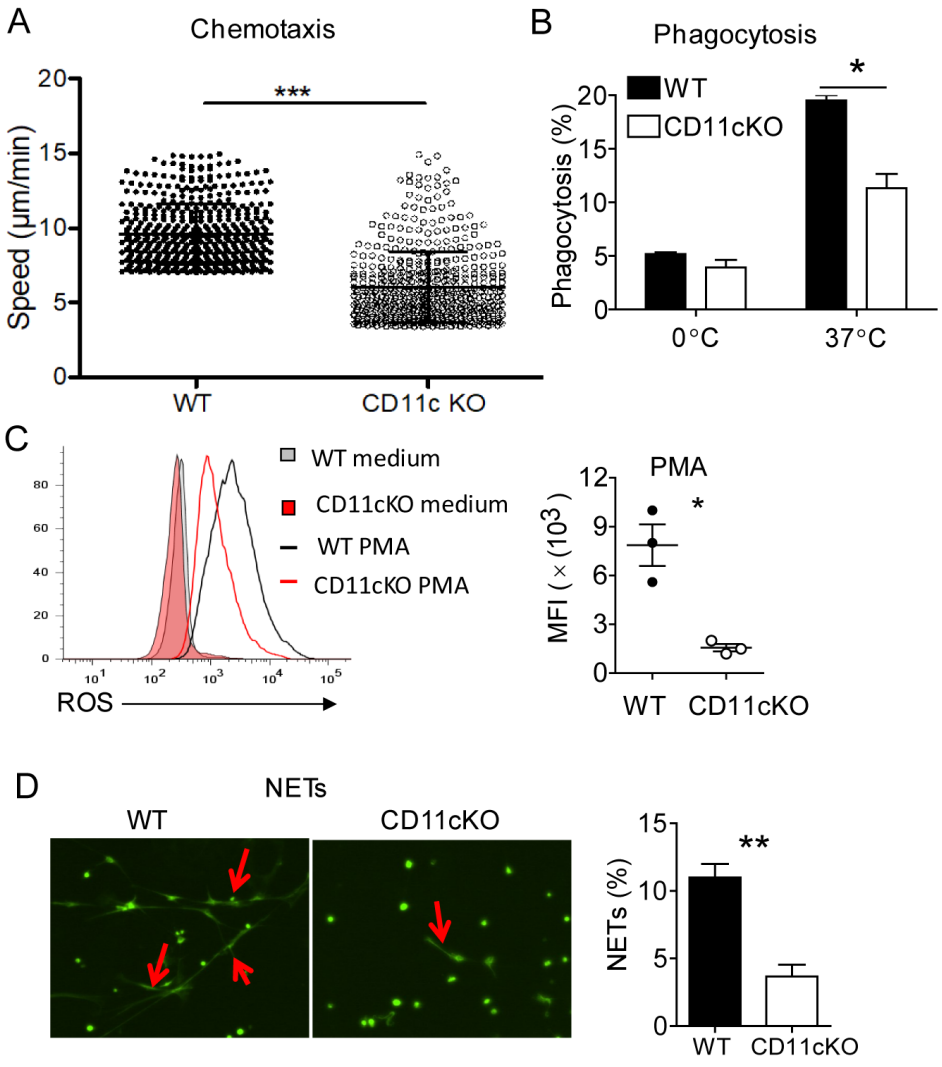

Supplemental Figure 4. CD11c deficiency impairs neutrophil functions. A, Neutrophil chemotaxis toward fMLP (1 μM) was examined using TAXIScan apparatus. Time-lapse image was obtained and analyzed with FIJI software. Chemotaxis speed was obtained. Data were shown as mean +/- S.D. Each dot represents one neutrophil. Statistical analysis was performed using Student's t-test. *** denotes P< 0.001. Data were representative of three independent experiments. **B**, Phagocytosis of opsonized FITC-*E. coli* was examined. Data were shown as mean +/- S.D. of phagocytosis % (n=3). Statistical analysis was performed using one-way ANOVA with *post hoc* Bonferroni analysis. *** P< 0.001. Two independent studies were performed. **C**, Neutrophil reactive oxygen species production was induced with PMA (100 nM) stimulation. The representative image of three independent experiments was shown. **D**, Neutrophil extracellular traps (NETs) formation was induced with PMA (50 nM) stimulation in WT and CD11c KO neutrophils. SYTOX green dye was used to detect DNA. Arrows indicated NETs. Nine independent experiments were performed.

Supplemental Figure 5.

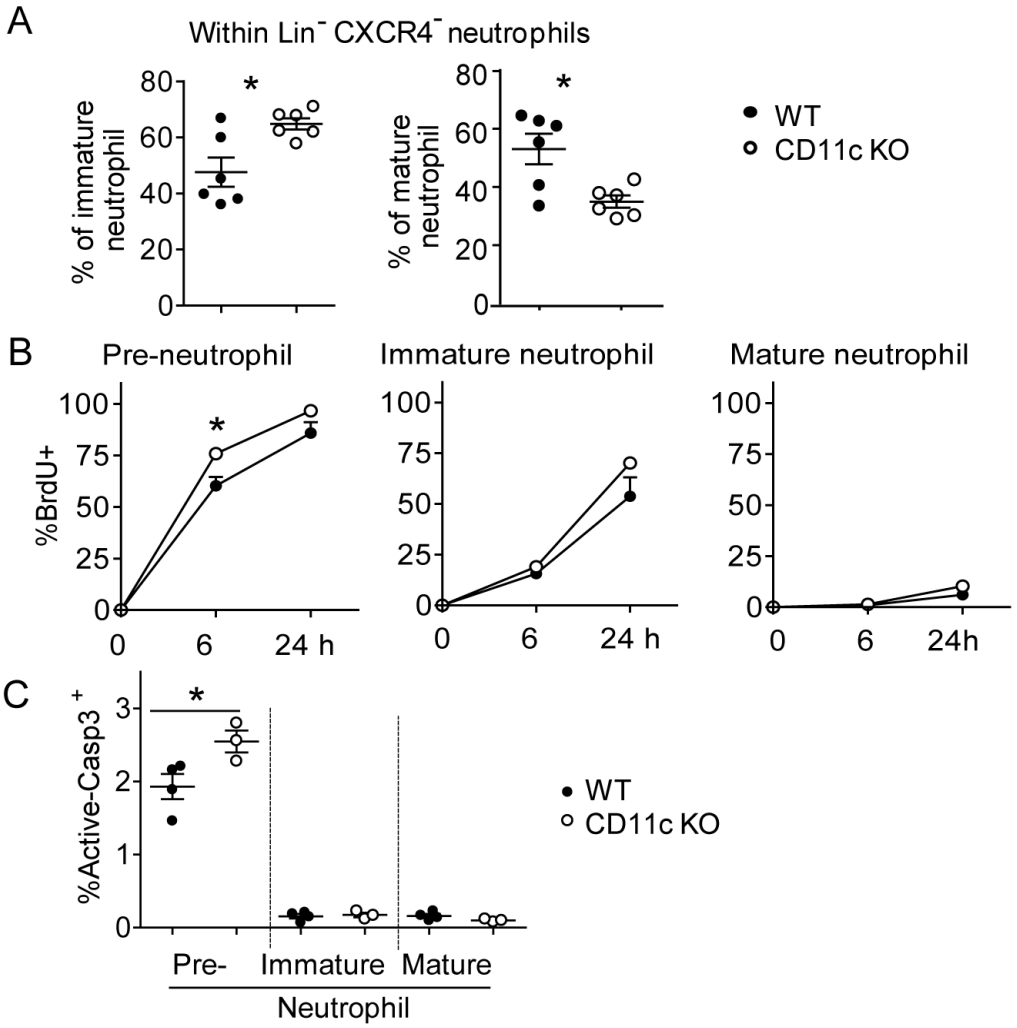

Supplemental Figure 5. CD11c affects neutrophil activities. **A**, Ratio of immature and mature neutrophils in the bone marrow of WT and CD11c KO mice. Depicted data are mean ± SD. Symbols indicate individual mouse. Three independent experiments were performed. **B**, Mice were injected *i.p.* with 1 mg of BrdU every 12 hours and sacrificed at indicated time points. N=3-5 in each time points. **C**, Active-caspase-3 detection by flow cytometry in pre-, immature- and mature-neutrophil. Data are representative of two experiments. Symbols represent individual mice. *$p<0.05$.

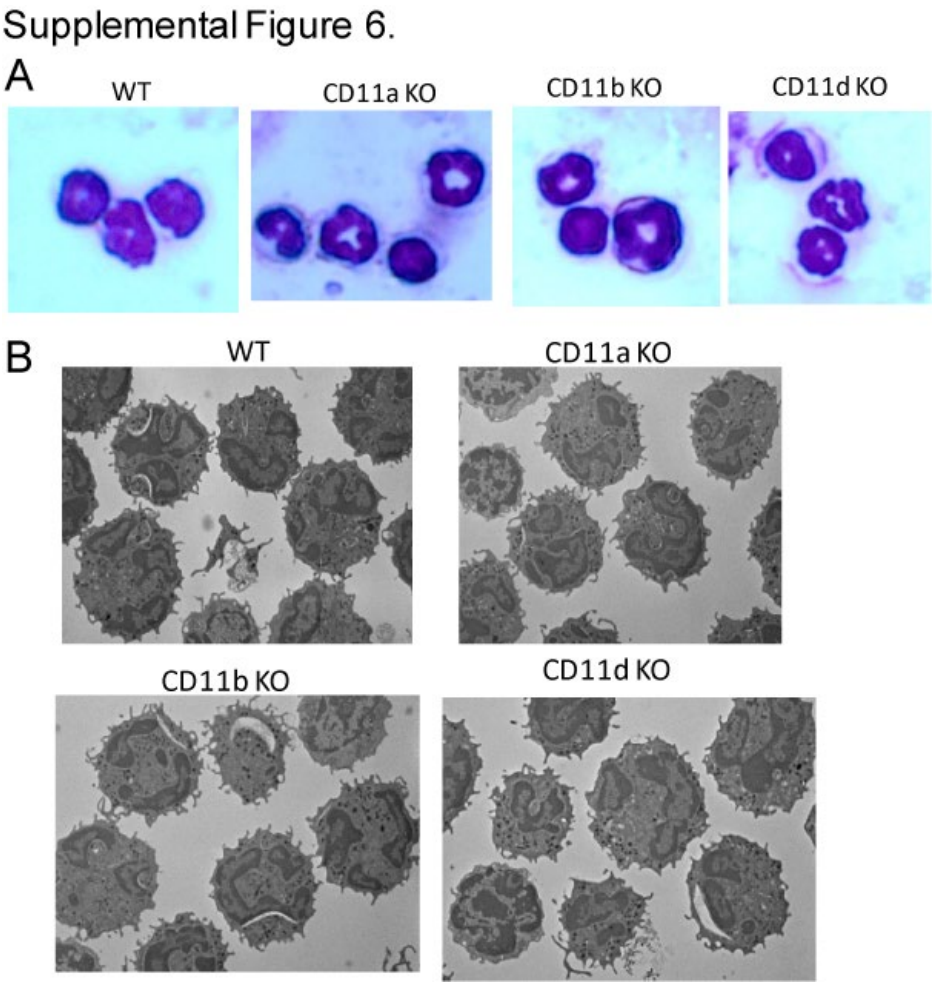

Supplemental Figure 6. The effect of β2 integrins in bone marrow neutrophil maturation. Bone marrow neutrophils of WT, CD11a KO, Cd11b KO, and CD11d KO mice were analyzed for neutrophil maturation by Giemsa staining (**A**) and EM (**B**). Representative image was shown. Neutrophils were enriched by gradient. No difference of lobulation observed among groups.

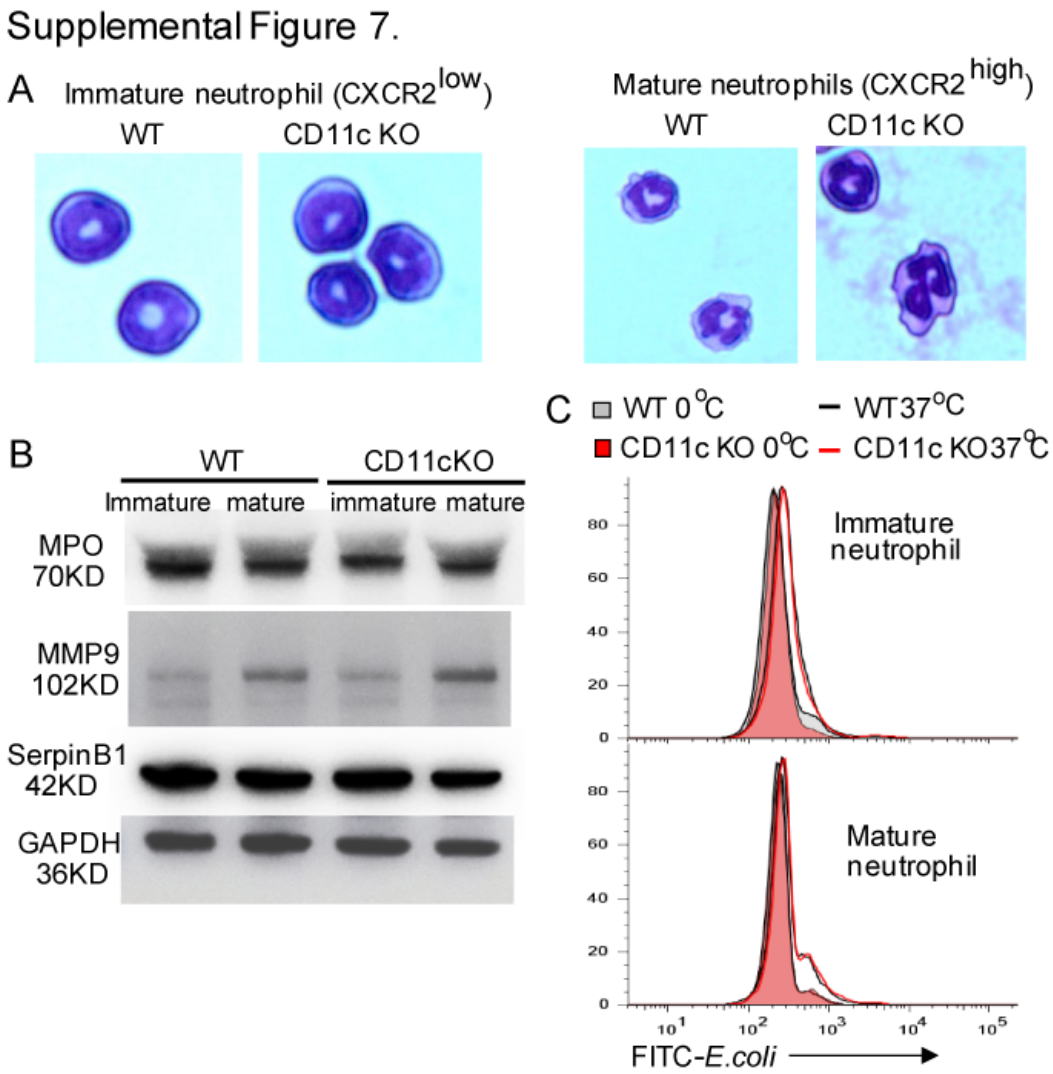

Supplemental Figure 7. Comparison of immature and mature neutrophils between WT and CD11c KO mice. A, Giemsa staining of sort-purified immature and mature neutrophils from WT and CD11c KO mice. Mature CD11c KO neutrophils exhibited comparable lobulation as WT ones. **B**, Western blot analysis of MPO, MMP-9, serpin B1 and GAPDH expression in WT immature and mature neutrophils and CD11c KO immature and mature neutrophils sorted by FACSAria system. **C**. FITC-labeled *E. coli* phagocytosis of sorted immature and mature neutrophils. Representative histograms were shown.

Supplemental Figure 8.

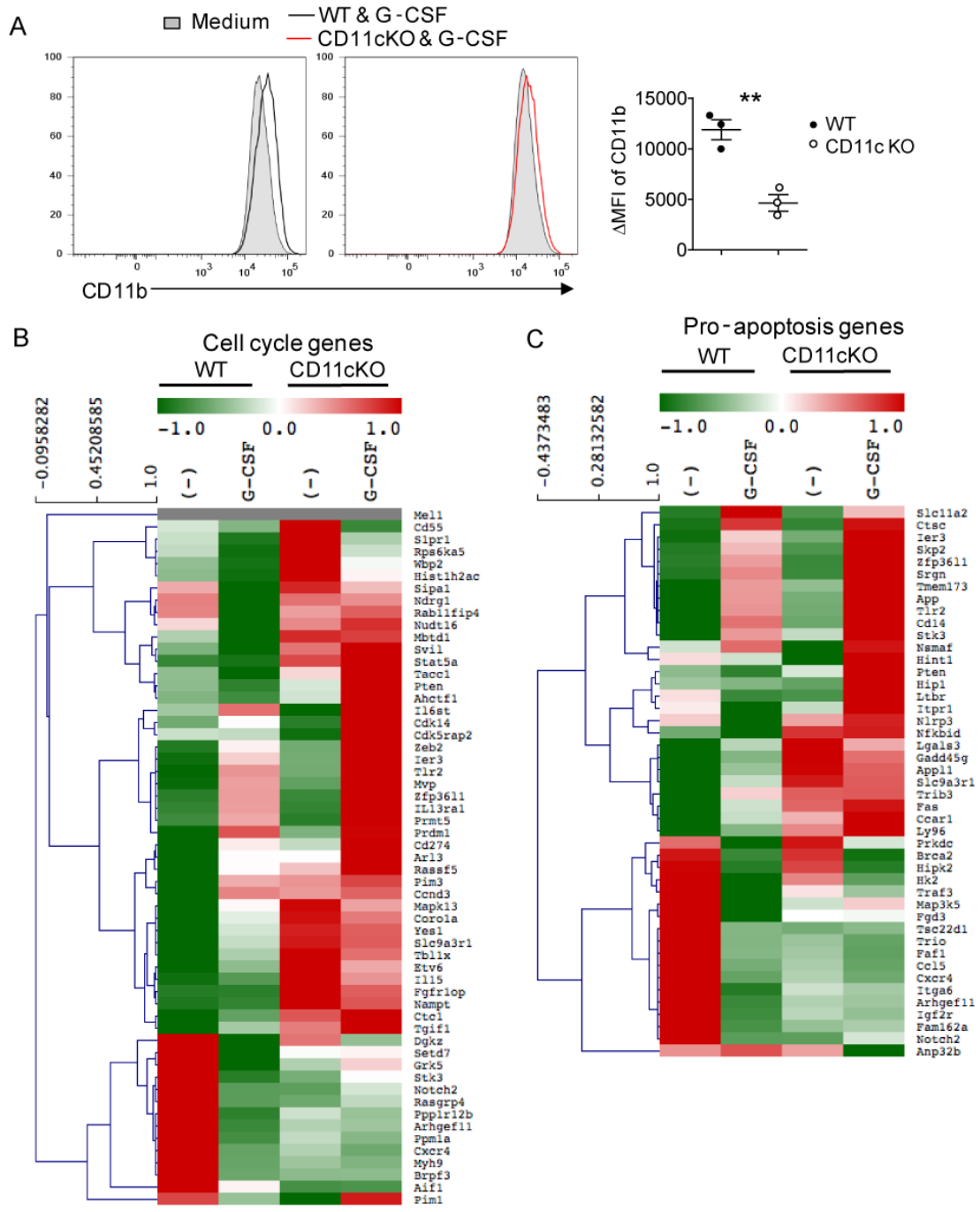

Supplemental Figure 8. CD11c KO pre/immature neutrophils upregulate cell cycle and pro-apoptosis genes under G-CSF. Both WT and CD11c KO pre/immature neutrophils were sorted by FACSAria system and cultured in the absence or presence of G-CSF (100ug/ml) for 24 hours. Cells were collected for flow cytometry analysis or bulk RNA sequencing analysis. **A**, surface CD11b expression increased by G-CSF. Shown are the flow cytometry overlay analysis. **B**, **C**. Expression heatmaps of cell cycle (**B**) and pro-apoptosis (**C**) related gene cluster retrieved from bulk RNAseq analysis.

Supplemental Figure 9.

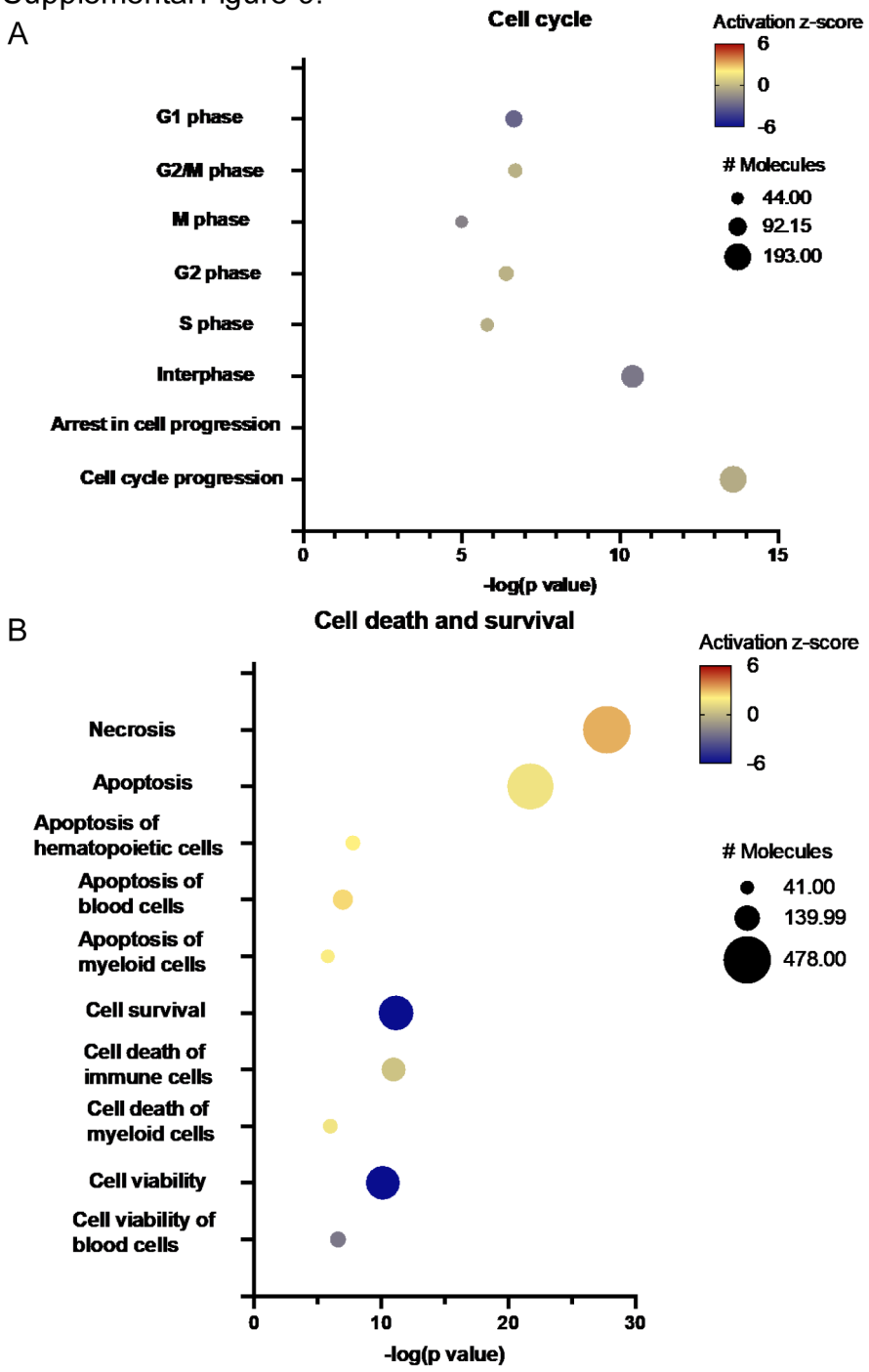

Supplemental Figure 9. Comparison of sorted WT and CD11c KO mature neutrophils' ontology Sorted bone marrow neutrophils from WT and CD11c KO mice were subjected to RNA seq analysis. Ontology analysis results of cell cycle genes (**A**) and cell death and survival genes (**B**) were presented on bubble plots following IPA pathway analysis. Bubble size represents the number of genes associated with each ontology.

Supplemental Figure 10.

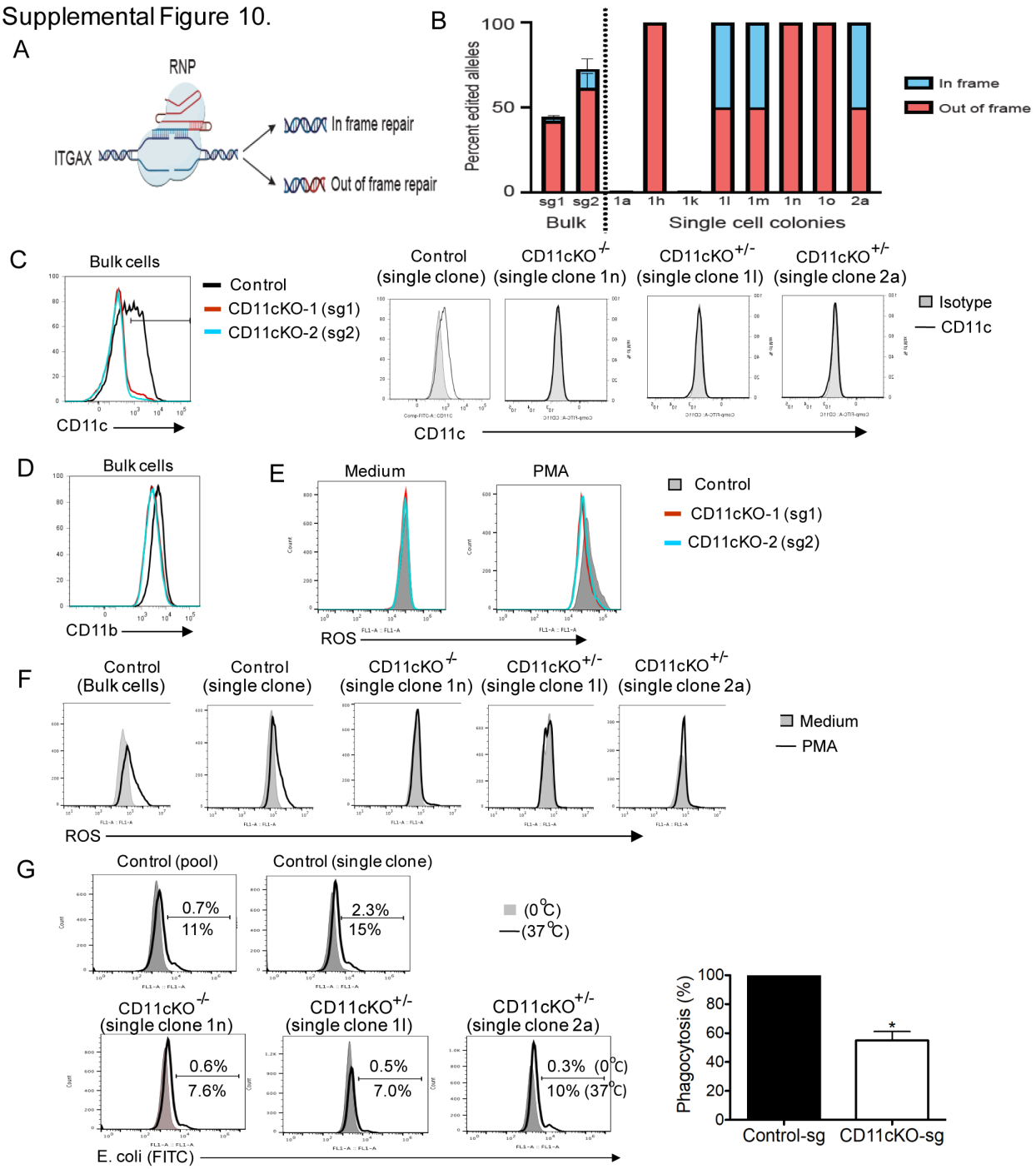

Supplemental Figure 10. CRISPR/Cas9 deletion of CD11c. A, Schematic of CRISPR editing of ITGAX by RNP delivery via nucleofection into HL-60 cells. CRISPR mediated double strand breaks can result in either in-frame or out-of-frame repair as depicted. **B**. Edited allele frequency of ITGAX in bulk HL-60 cells after RNP delivery of sg1 or sg2 (left) or in single-cell derived colonies [17]. Colonies were either homozygous wild type (1a, 1k), homozygous knockout (1h, 1n, 1o), or compound heterozygous with one out of frame edit and one in-frame edit (1l, 1m, 2a). No heterozygous colonies were isolated. **C,** CD11c deletion via CRISPR/Cas9 verified by flow cytometry-based CD11c expression analysis in bulk cells (left) and single clone cells [17], **D**,

CD11b expression on control and CD11c KO HL-60 cell-differentiated neutrophils. **E**, ROS generation in control and CD11c KO HL-60 cell-differentiated neutrophils upon PMA stimulation (100 nM). **F**, ROS generation on control (bulk cells and single clone) and three single clones of CD11c KO HL-60 cell-differentiated neutrophils upon PMA stimulation (100 nM). **G**, phagocytosis of control (bulk cells and single clone) and three single clones of CD11c KO HL-60 cell-differentiated neutrophils. **F**-**H**. shown are representative data from three independent experiments with the same pattern. For phagocytosis (G), we also presented the ratio of CD11c KO-sg transfected cells' phagocytosis compared to control-sg transfected cells. Student t test was used for statistical analysis. * $p<0.05$.

Supplemental figure 11.

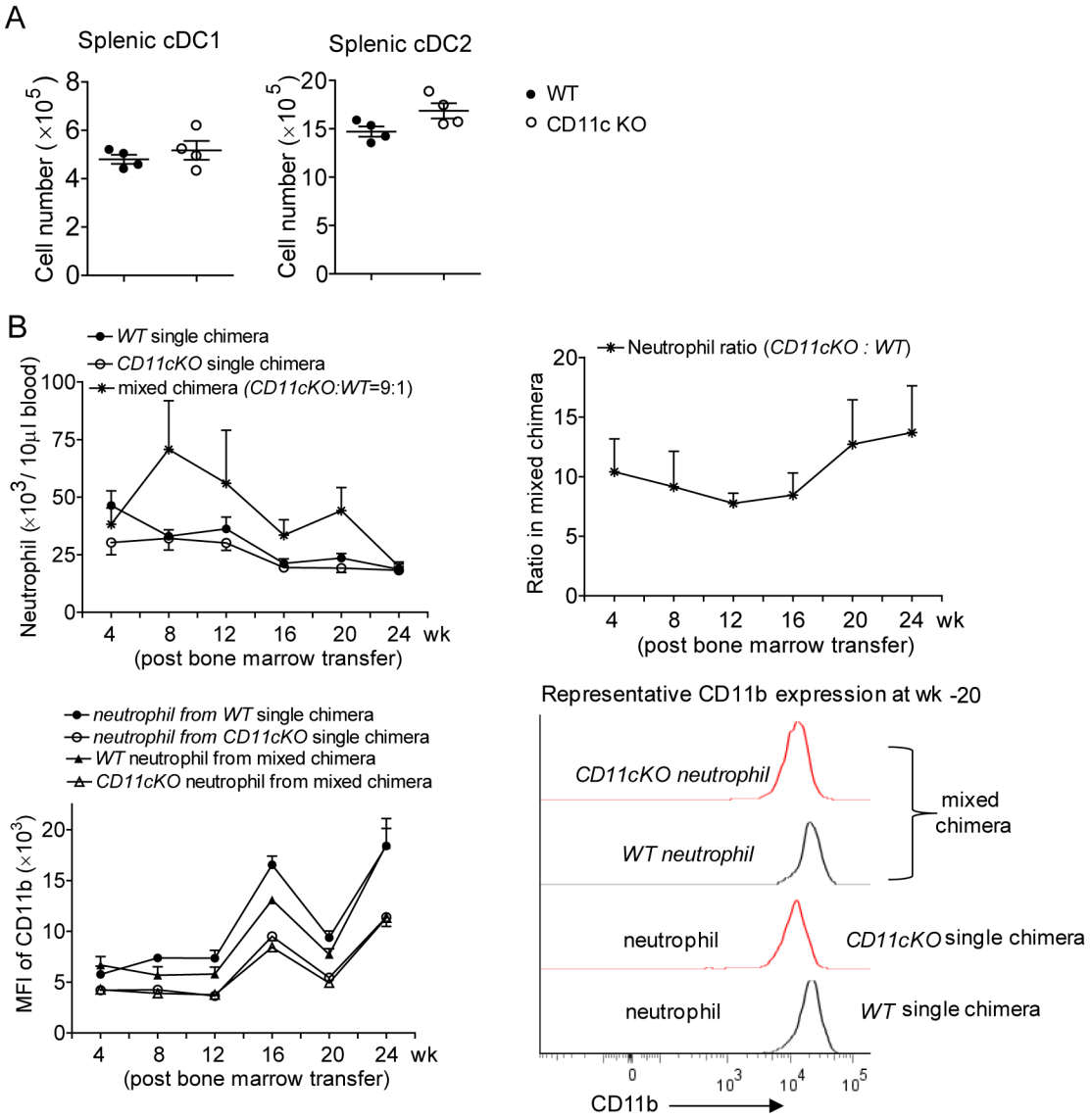

Supplemental Figure 11. Dendritic cell counting and bone marrow chimera. A. Spleens from age- and gender- matched WT and CD11cKO mice were digested, washed, subjected to red blood cell lysis, and prepared into single cell suspension. cDC1 and cDC2 subsets were counted according to the description in Supplemental Figure 1A. Experiment was repeated twice with same pattern. B. Bone marrow cells from CD11cKO (CD45.2) and WT (CD45.1) were transferred into lethally irradiated recipient B6 mice separately (single chimera) or together at the ratio of 9:1 (mixed chimera). Four weeks later, recipient mice were monitored for blood neutrophil number (up panels) and CD11b expression (bottom panels: bottom-left showing the CD11b MFI over 24 weeks; bottom-right showing the representative overlay analysis of CD11b expression at 20 weeks post bone marrow transplantation). Each group contains four mice.

Supplemental figure 12.

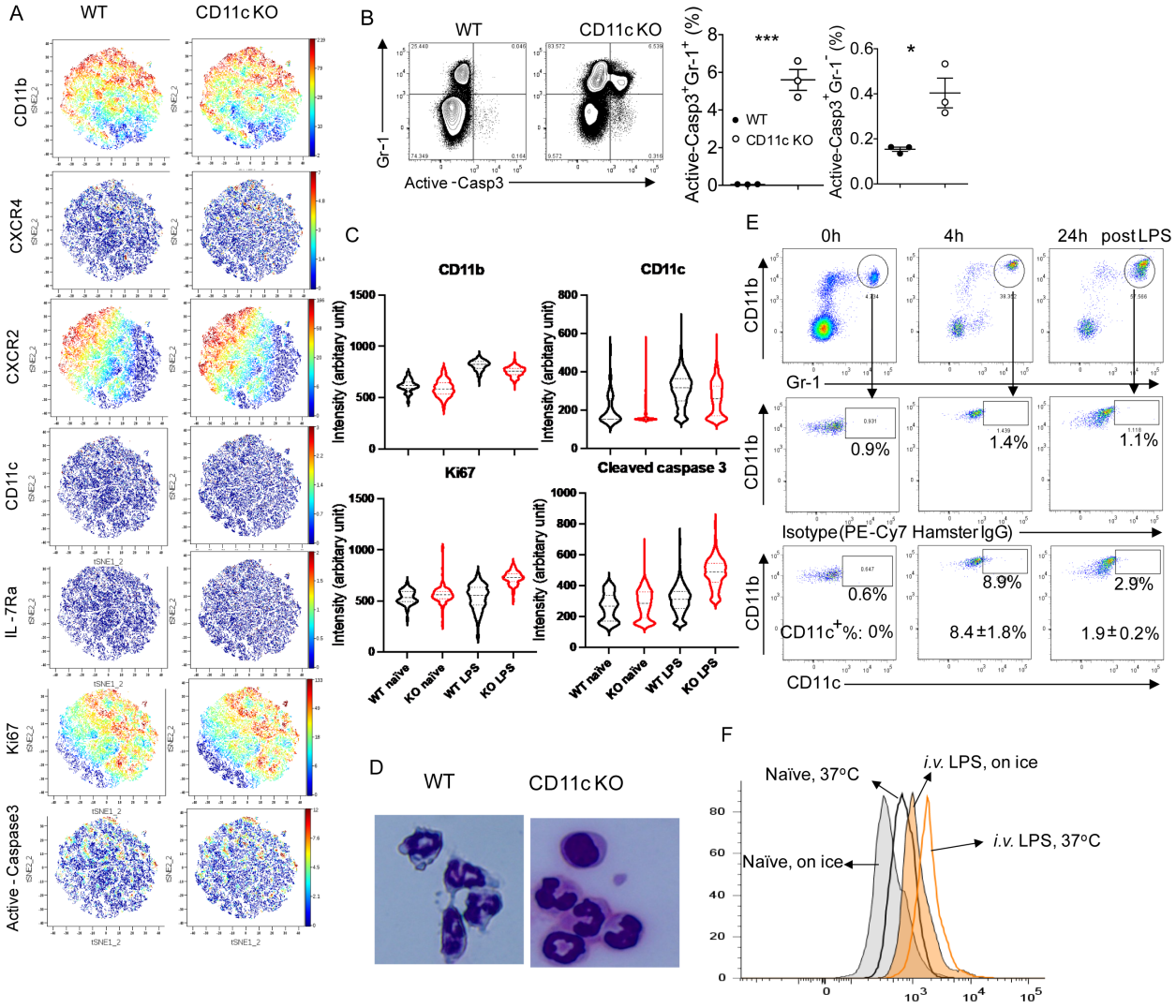

Supplemental Figure 12. CD11c deficiency affects neutrophil cell death and proliferation. **A**, CyTOF analysis of bone marrow-derived neutrophils isolated from naïve WT and CD11c KO mice. **B**, Flow cytometry analysis confirming the active-caspase 3 level of neutrophils from WT and CD11cKO mice at 6 hours post *i.v.* LPS injection. Left: representative flow cytometry picture; Right: statistical analysis. One symbol represents an individual mouse. Experiments were repeated at least 3 times with similar pattern. **C**. Violin plot of CD11b, CD11c, Ki67, and cleaved caspase 3 expression of bone marrow derived neutrophils isolated from LPS injected WT and CD11c KO mice in CyTOF analysis. **D**, Giemsa staining of bone marrow neutrophils post *E. coli i.p.* injection. Shown are representative pictures of three biological samples. **E**. CD11c expression on blood neutrophils after *i.v.* LPS injection. WT mice were i.v. injected with LPS (10 mg/kg), and peripheral blood were collected at various time point as indicated. Neutrophil staining (top panel) and their CD11c expression (bottom panel) over time were monitored by flow cytometry. Isotype control was strictly applied in the experiment (middle panel). CD11c-positive ratio was calculated by subtracting the isotype control. Experiment was repeated twice with the same pattern. **F**. Function analysis of blood neutrophils upon *i.v.* LPS

injection. At 4 hours post *i.v.* LPS injection, blood was collected. In parallel, blood from naïve WT mice was collected as control. Whole blood was labelled with dihydrorhodamine 123 (DHR) for 5 min at 37°C, washed, and resuspended in complete RPMI-1640 containing 10% FBS, FcR blocker, APC-CD11b and pacific blue-Ly6G, and further incubated either on ice or in 37°C water bath for additional 15 min. At the end of incubation, whole blood was subjected to red-blood-cell-lysis, washed and then directly analyzed by FACSCanto. ROS generation was measured by gating on neutrophil ($CD11b^{+}Ly6G^{+}$). Shown are representative data of three independent experiments with the same pattern.

Supplemental figure 13.

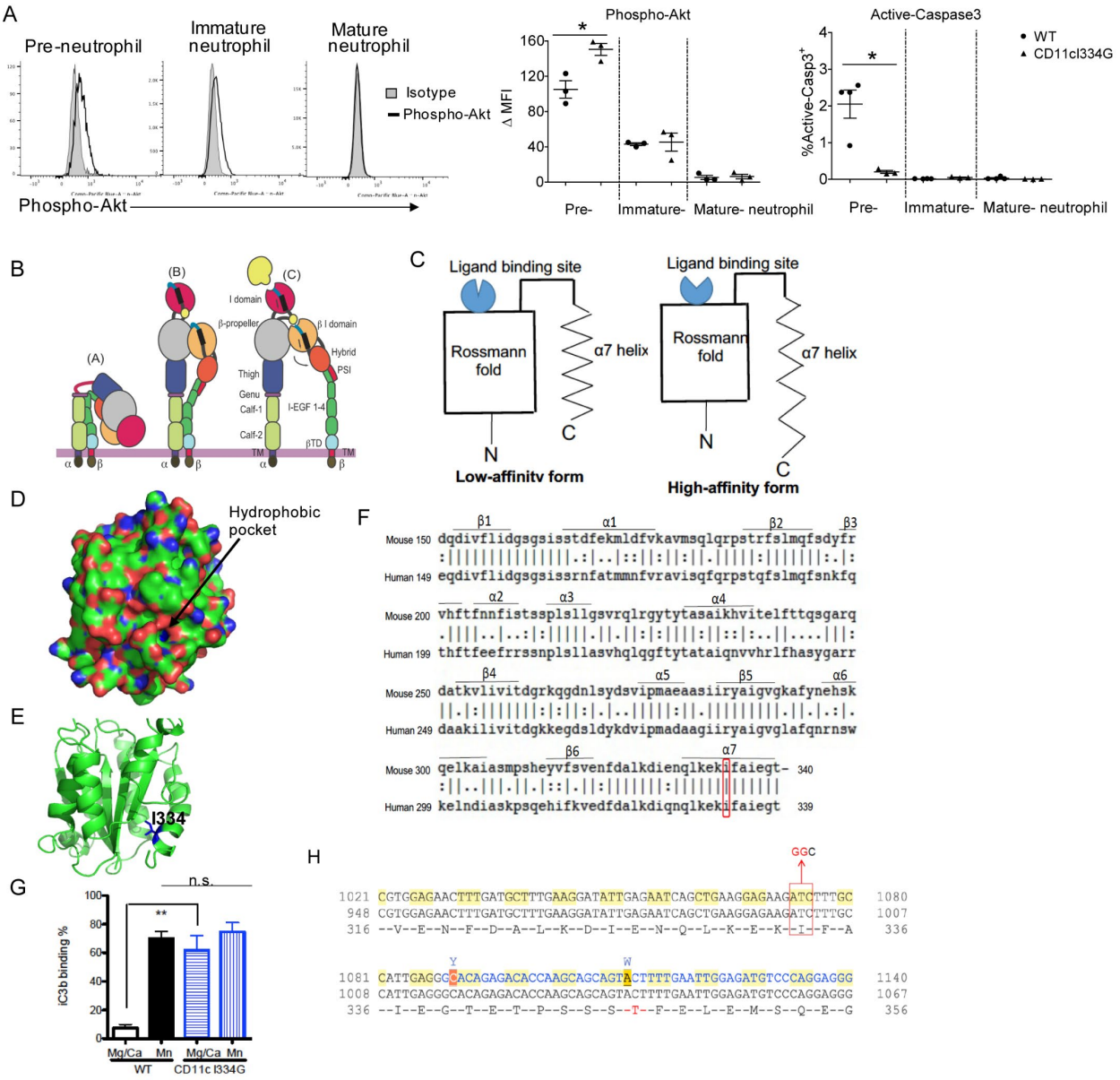

Supplemental Figure 13. CD11c I334G knock-in mice A. Phospho-flow detecting Akt activation. Bone marrow cells were isolated and surface stained, fixed, permeabilized and intracellularly stained with anti-phospho-Akt antibody. Left: representative flow cytometry overlay analysis; Middle: p-Akt levels in different neutrophil subsets from both WT and CD11cI334G-KI mice. ΔMFI calculated by subtracting the MFI from corresponding isotype control staining. Symbols represent individuals, experiments were repeated twice with the same pattern; Right: active-Caspase3 levels in different neutrophil subsets from both WT and CD11cI334G-KI mice. * P< 0.05, *** P< 0.001. Symbol represents an individual mouse. **B**. Schematic demonstration of conformational changes of CD11c (α subunit) /CD18 (β subunit). Inactivated (closed) state (A), intermediate state (B) and activated (open) state (C). Ligand (yellow) binds to the ligand binding domain (I domain) only at the activated state. **C**. The scheme of the ligand binding domain (I domain). The ligand binding site is closed when the α7 helix is not unwinded, but it becomes open when the helix is unwinded. **D**. Predicted mouse I

domain by I-TASSER (Iterative threading Assembly refinement) software and the hydrophobic pocket involving the α7 helix. **E**. Predicted mouse I domain structure and Ile-334 located at the hydrophobic pocket. **F**. The alignment of murine and human CD11c I domain alignment. **G**. The binding of mouse CD11c WT and CD11c I334G transiently transfected HEK cells to iC3b. Mean +/- S.D. of three replicates. ** P< 0.01. G. Point mutation to make CD11c I334G mutant. **H**. Sequence of CD11c I334G KI mice.

Supplemental figure 14.

ID		Protein name	Granule presence
P07237	PDIA1 (P4HB)	Protein disulfide-isomerase	
P30101	PDIA3	Protein disulfide-isomerase A3	GE, SG
Q01518	CAP1	Adenylyl cyclase-associated protein 1	
P08133	ANXA6	Annexin A6	
P08238	HS90B (HSP90AB1)	Heat shock protein HSP 90-beta	
P11021	BIP (HSPA5)	Endoplasmic reticulum chaperone BiP	GE, SG
P11142	HSP7C	Heat shock cognate 71 kDa protein	
P12956	XRCC6	X-ray repair cross-complementing protein 6	
P13667	PDIA4	Protein disulfide-isomerase A4	
P13796	PLSL (LCP1)	Plastin-2	GE, SG, AZ
P26038	MOES (MSN)	Moesin	SP
P38646	GRP75 (HSPA9)	Stress-70 protein, mitochondrial	
P55072	TERA (VCP)	Transitional endoplasmic reticulum ATPase	
O43707	ACTN4	Alpha-actinin-4	
P12814	ACTN1	Alpha-actinin-1	GE, SG
P14625	ENPL (HSP90B1)	Endoplasmin	
P14923	PLAK (JUP)	Junction plakoglobin	
P15924	DESP (DSP)	Desmoplakin	GE, SG
P46940	IQGA1 (IQGAP1)	Ras GTPase-activating-like protein IQGAP1	GE
P06576	ATPB (ATP5F1B)	ATP synthase subunit beta. Mitochondrial	GE, SG
P14618	KPYM (PKM)	Pyruvate kinase PKM	
P68363	TBA1B (TUBA1B)	Tubulin alpha-1B chain	GE, SG, AZ
P68371	TBB4B (TUBB4B)	Tubulin alpha-4B chain	
P78371	TCPB (CCT2)	T-complex protein 1 subunit beta	
P35579	MYH9	Myosin-9	GE, SG, AZ
Q00610	CLH1 (CLTC)	Clathrin heavy chain 1	SG
P27797	CALR	Calreticulin	GE, SG
P50990	TCPQ (CCT8)	T-complex protein 1 subunit theta	
P17987	TCPA (TCP1)	T-complex protein 1 subunit alpha	
Q02413	DSG1	Desmoglein-1	GE, SG
P49736	MCM2	DNA replication licensing factor MCM2	
P07237	PDIA2	Protein disulfide-isomerase	
P19338	NUCL (NCL)	Nucleolin	

GE, gelatinase; SG, specific; AZ, azurophil

Supplemental Figure 14. Proteomics analysis of CD11c binding targets.
The list of proteins with top score is shown. The presence of each protein in neutrophil granules was referred to the paper by Lominadez et al (reference 43 in the manuscript text).

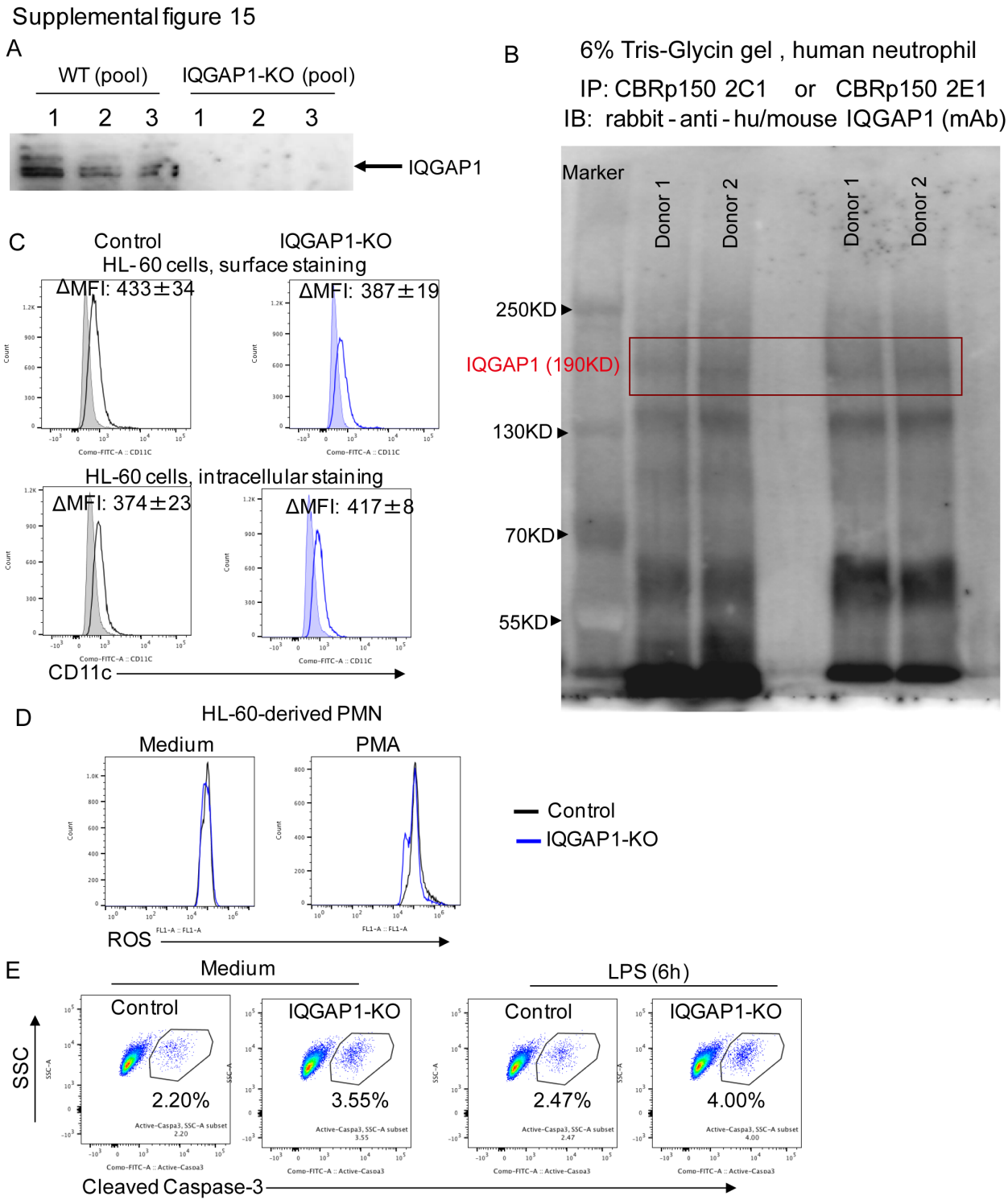

Supplemental Figure 15. Verification of IQGAP1 deletion in HL-60 cells.
A. IQGAP-1 KO HL-60 cells were derived by CRISPR/Cas9 knockout and subjected to Western blot analysis. Western blot image confirming the successful knockout. **B**. Neutrophils from peripheral blood of two donors were enriched by using Polymorphprep™ (resulting purity > 90%). Purified neutrophils were lyzed by RIPA buffer in the presence of protease inhibitors and

incubated with two anti-human CD11c antibodies (clone CBRp150 2C1 or clone CBRp150 2E1) overnight at 4°C, followed by incubation with ProteainA&G agarose beads. Then the beads were collected, washed, and boiled with SDS sample buffer, and IQGAP-1 was probed by western blot analysis. CD11c bound to IQGAP1 in human neutrophils. **C**. Cell surface and intracellular CD11c expression in IQGAP1 KO HL-60 cells. **D**. ROS generation in control and IQGAP1 KO HL-60 cell-differentiated neutrophils upon PMA stimulation (100 nM). Shown are representative overlay analysis of three cell pools for each genotype. Experiments were repeated three times with exactly same pattern. **E**. Cleaved caspase-3 expression in control and IQGAP1 KO HL-60 cell-differentiated neutrophils with or without LPS. Shown are representative overlay analysis of three cell pools for each genotype. Experiments were repeated three times with exactly the same pattern.

Supplemental Table 1. List of selected downregulated genes in CD11c KO mature neutrophils

Downregulated cell cycle genes
CDK2-associated protein 1 (Cdk2ap1)
DBF4 zinc finger (Dbf4)
EP300 interacting inhibitor of differentiation 1 (Eid1)
KH domain containing RNA binding, signal transduction associated 1 (khdrbs1)
M-phase specific PLK1 interacting protein (Mplkip)
MAP/microtubule affinity regulating kinase 4 (Mark4)
SAC domain containing 1 (Sac3d1)
WT1 associating protein (Wtap)
Cell division cycle 34 (Cdc34)
Centromere protein V (Cenpv)
Cyclin A2 (Ccna2)
Cyclin G2 (Ccng2)
Fizzy and cell division cycle 20 related 1(Fzr1)
Guanine nucleotide binding protein (G protein), alpha inhibiting 2 (Gnai2)
Kelch-like 9 (Klhl9)
Nuclear protein transcriptional regulator 1 like (Nupr1l)
Protein kinase, membrane associated tyrosine/threonine 1 (Pkmyt1)
Protein phosphatase 1 catalytic subunit gramma (Ppp1cc)
Ribonucleic acid export (Rae1)
Ubiqutin-conjugating enzyme E2S (Ube2s)
V-ral simian leukemia viral oncogene A (ras related)(Rala)

Downregulated cell death related genes
B cell CLL/lymphoma 7C (Bcl7c)
BCL2-antagonist/killer (Bak1)
BCL2-associated athanogene 1 (Bag1)
Harvery rat sarcoma virus oncogene (Hras)
TM2 domain containing 1 (Tm2d1)
X-box binding protein (Xbp1)
Y box protein 3 (Ybx3)
Apoptosis, caspase activation inhibitor (Aven)
Complement component 1, q subcomponent binding protein (C1qbp)
Etoposide induced 2.4 mRNA (Ei24)
Intraflagellar transport 57 (Ift57)
Mitochondorial carrier 1 (Mtch1)
Mitogen-activated protein kinase kinase 7 (Map2k7)
Peptidylprolyl isomerase F (cyclophillin F) (Ppif)
Pleckstrin homology like domain, family A, member 1 (Phlda1)
Programmed cell death 4 (Pdcd4)
Ras homolog family member B (Rhob)
Riboflavin kinase (Rfk)
Superoxide dismutase 1, soluble (Sod1)
Suppressor of defective silencing 3 homolog (S. cervisiase) (Suds3)
Yippee like 3 (Ypel3)

References

1. Gupta D, Shah HP, Malu K, Berliner N, Gaines P. Differentiation and characterization of myeloid cells. *Curr Protoc Immunol.* 2014;104:22F 25 21-22F 25 28.
2. Carrigan SO, Weppler AL, Issekutz AC, Stadnyk AW. Neutrophil differentiated HL-60 cells model Mac-1 (CD11b/CD18)-independent neutrophil transepithelial migration. *Immunology.* 2005;115(1):108-117.
3. Bak RO, Dever DP, Porteus MH. CRISPR/Cas9 genome editing in human hematopoietic stem cells. *Nat Protoc.* 2018;13(2):358-376.
4. Bao EL, Nandakumar SK, Liao X, et al. Inherited myeloproliferative neoplasm risk affects haematopoietic stem cells. *Nature.* 2020;586(7831):769-775.
5. Vaidyanathan S, Salahudeen AA, Sellers ZM, et al. High-Efficiency, Selection-free Gene Repair in Airway Stem Cells from Cystic Fibrosis Patients Rescues CFTR Function in Differentiated Epithelia. *Cell Stem Cell.* 2020;26(2):161-171 e164.
6. Boettcher S, Gerosa RC, Radpour R, et al. Endothelial cells translate pathogen signals into G-CSF-driven emergency granulopoiesis. *Blood.* 2014;124(9):1393-1403.
7. Carbo C, Duerschmied D, Goerge T, et al. Integrin-independent role of CalDAG-GEFI in neutrophil chemotaxis. *J Leukoc Biol.* 2010;88(2):313-319.
8. Pro CI, Yealy DM, Kellum JA, et al. A randomized trial of protocol-based care for early septic shock. *N Engl J Med.* 2014;370(18):1683-1693.
9. Helft J, Bottcher J, Chakravarty P, et al. GM-CSF Mouse Bone Marrow Cultures Comprise a Heterogeneous Population of CD11c(+)MHCII(+) Macrophages and Dendritic Cells. *Immunity.* 2015;42(6):1197-1211.
10. Sen M, Yuki K, Springer TA. An internal ligand-bound, metastable state of a leukocyte integrin, alphaXbeta2. *J Cell Biol.* 2013;203(4):629-642.
11. Vorup-Jensen T, Ostermeier C, Shimaoka M, Hommel U, Springer TA. Structure and allosteric regulation of the alpha X beta 2 integrin I domain. *Proc Natl Acad Sci U S A.* 2003;100(4):1873-1878.
12. Xiong JP, Li R, Essafi M, Stehle T, Arnaout MA. An isoleucine-based allosteric switch controls affinity and shape shifting in integrin CD11b A-domain. *J Biol Chem.* 2000;275(49):38762-38767.
13. Li Y, Evers J, Luo A, Erber L, Postler Z, Chen Y. A Quantitative Chemical Proteomics Approach for Site-specific Stoichiometry Analysis of Ubiquitination. *Angew Chem Int Ed Engl.* 2019;58(2):537-541.
14. Cox J, Mann M. MaxQuant enables high peptide identification rates, individualized p.p.b.-range mass accuracies and proteome-wide protein quantification. *Nat Biotechnol.* 2008;26(12):1367-1372.
15. Cox J, Neuhauser N, Michalski A, Scheltema RA, Olsen JV, Mann M. Andromeda: a peptide search engine integrated into the MaxQuant environment. *J Proteome Res.* 2011;10(4):1794-1805.
16. McCaffrey PG, Jain J, Jamieson C, Sen R, Rao A. A T cell nuclear factor resembling NF-AT binds to an NF-kappa B site and to the conserved lymphokine promoter sequence "cytokine-1". *J Biol Chem.* 1992;267(3):1864-1871.
17. Wright HL, Thomas HB, Moots RJ, Edwards SW. RNA-seq reveals activation of both common and cytokine-specific pathways following neutrophil priming. *PLoS One.* 2013;8(3):e58598.